188. Peptide Conformation from Coupling Constants: Scalar Couplings as Restraints in MD Simulations

by **Matthias Eberstadt, Dale F. Mierke, Matthias Köck,** and **Horst Kessler***

Organisch-chemisches Institut, Technische Universität München, Lichtenbergstrasse 4, D–8046 Garching

(10.VIII.92)

The question of how far one can go in the determination of conformation with the sole use of coupling constants as restraints in MD simulations was addressed. Couplings are being used ever more frequently as constraints as measuring heteronuclear long-range coupling constants becomes easier. For this investigation, cyclosporin A, which has previously been extensively examined with NOE-restrained simulations, is used as a model system. Many additional one- and three-bond coupling constants have been measured. The MD simulations were carried out with the addition of a potential-energy penalty function based directly on the *Karplus* curve. It is shown that, for dihedral angles with more than one coupling, the restraints are very efficient, in agreement with the structure observed from NOEs. However, it turned out that the structure of CsA is not adequately described, when only J couplings are used.

Introduction. – Recently, there has been increased interest in the use of coupling constants in conformational analysis. This has come about mainly because of the increased use of isotopically labeled proteins, which greatly simplifies the measurement of heteronuclear coupling constants. The additional couplings remove the ambiguities arising from the *Karplus* equation used to convert couplings to dihedral angles [1]. Such methods have long been in use for the unambiguous assignment of diastereotopic protons [2] which is important for increasing the quality and resolution of peptide and protein structures [3]. For systems, in which isotopic enrichment is not feasible, methods efficient in natural abundance have been devised [4].

The backbone conformation of peptides and proteins is described by the ϕ and ψ torsions (assuming a peptide bond with $\omega = 180°$). The ϕ angle is defined by several heteronuclear couplings including ^3J(HN–Cβ), ^3J(HN–C′), or ^3J(Hα(i)–C′(i – 1)) and the homonuclear ^3J(HN–Hα) coupling constant. Hence, the ϕ angle is well determined with up to four couplings. On the other hand, the ψ angle is defined by only two heteronuclear couplings, ^3J(N(i)–Hα(i – 1)) and ^3J(N(i)–Cβ(i – 1)), which are difficult to obtain in natural abundance. To overcome this problem, we have recently investigated the use of the one-bond coupling between the α-C-atom and proton, ^1J(Cα–Hα), [5] which has been previously shown to depend on both the ϕ and ψ dihedral angles [6]. The combined use of several coupling constants in restrained MD calculations might be used to improve the quality of a NOE-derived structure or in extreme cases, to determine a structure based solely on coupling constants.

Penalty terms for the one- and three-bond couplings have recently been implemented into a molecular-dynamics-simulation program [7]. The method utilizes the direct application of the *Karplus* equation [1] so that no assumptions have to be made for allowed ranges of dihedral angles, a problem encountered with dihedral angle restraining [8].

Simulations with this penalty function has been shown to be quite effective in generation of structures consistent with the experimental data.

Here, we address the question of how far one can go in structure determination with coupling constants alone. The model system used in this study is Cyclosporin A (CsA), an undecapeptide which has been extensively studied by NMR [9]. This is a good test system because it shows one predominant, well defined conformation in $CHCl_3$ and 62 coupling constants have been measured.

Experimental Methods. – *NMR Investigations.* All measurements were carried out on a sample of CsA containing 50 mg in 0.5 mol of $CDCl_3$ (83 mmol·l^{-1}). The sample was vacuum-sealed after five freeze-thaw-pump cycles. The sample was not spun. All experiments were run at 300 K. The heteronuclear long-range coupling constants were determined using a TOCSY with ω_1-hetero-half-filter [4] and a modified HMBC [10]. Heteronuclear ^1J(C,H) coupling constants between H(α) and C(α) were extracted from a HMQC spectrum without decoupling during acquisition [11]. The TOCSY spectrum with ω_1-hetero-half-filter was recorded with 2048 data points in F_2, 240 scans per experiment and a sweep width of 4545 Hz in both dimensions. The BIRD sequence [12] was employed to enable fast pulse repetition rates by suppressing ^{12}CH pairs [13]. The mixing time of the MLEV-17 [14] sequence was 80 ms. The HMBC [15] was carried out with a delay 80 ms, to allow for the evolution of heteronuclear long-range couplings. The spectral widths were 12,800 and 4500 Hz in the F_1 and F_2 dimensions, respectively. In the F_1 dimension, the C=O signals were folded after careful inspection of the ^{13}C spectrum [16]. The reference TOCSY spectrum was recorded using DIPSI-2 [17] placed inside a z-filter [18] for mixing (see *Experimental*). The HMQC spectrum was recorded with 1024 data points and 230 increments. The ^1J(Cα–Hα) coupling constants were extracted from the F_2 dimension of the appropriate slices and zero-filled to a size of 16,384 data points, resulting in a digital resolution of 0.27 Hz/point.

Molecular-Dynamics Calculations. a) *Scalar Coupling as Restraints.* The application of the constraints from the coupling constants has been previously described [7]. The penalty function is similar to that commonly used for NOE restraints:

$$E_J = \tfrac{1}{2}\, k_J\, (J - J_{exp})^2 \tag{1}$$

where k_J is the force constant, E_J is the energy of the penalty function, J and J_{exp} are the coupling constants calculated from the dihedral angle and the experimental value, respectively. The coupling constant is calculated from the dihedral subtended by the coupled atoms, Θ, using the *Karplus* equation [1a, b]:

$$^3J = A \cos^2\Theta + B \cos\Theta + C \tag{2}$$

where the coefficients A, B, and C have been empirically adjusted for dihedral torsions involving different atoms [1c] [19]. The curve utilized for the ^1J(Cα–Hα) couplings was taken from *Egli* and *Philipsborn* [6]:

$$^1J = A + B \cos^2(\phi + 30°) + C \cos^2(\psi - 30°) \tag{3}$$

appropriate for L-amino acids.

b) *$CHCl_3$ as a Solvent in MD Simulations.* The simulations were carried out in $CHCl_3$, with the solvent described as a four-point model using a united atom for the C-atom and

proton. The solvent is considered rigid with the geometry (described by distances of 0.172 and 0.283 nm between CH–Cl and Cl–Cl, respectively) maintained by the application of SHAKE [20]. The charges and *Lennard-Jones* parameters were taken from the work of *Jørgensen* and coworkers [21]. An equilibrated box of dimethyl sulfoxide (also treated as four points) [22] was used as a starting configuration for the $CHCl_3$, with the O-atoms and two methyl C-atoms of DMSO replaced by Cl-atoms. The correct geometry of the solvent was obtained by energy minimization. The box was then scaled to obtain the correct density of $CHCl_3$ and an MD simulation of 200 ps carried out to equilibrate the $CHCl_3$ solution. The final coordinate set from this simulation was used for the solvent simulations of CsA.

c) *Computer Simulations of CsA.* MD simulations of CsA using two different starting structures were carried out. The first started from a well refined structure from a previous restrained MD simulation using 117 NOEs [9]. This simulation was to examine the effects of adding the scalar coupling constants as restraints. The other simulation started from a structure well removed from the conformation found in solution, with only coupling constants used as restraints. The molecular-dynamics simulations were carried out with the GROMOS program [23]. The peptide was placed in a periodic truncated octahedron of 38.4 nm^3 containing 130 $CHCl_3$ solvent molecules. A step size of 2 fs employing the SHAKE algorithm [20] was used with the nonbonded interactions updated every 25 steps with a cut-off radius of 1.0 nm. The simulations were run at 1000 K with a tight coupling to a temperature bath [24] (a relaxation time of 20 fs) for a equilibration period of 20 ps. This temperature was reduced to 300 K, the coupling was relaxed (200 fs) and the simulation continued for 60 ps. The force constant was set to 2000 $kJ \cdot mol^{-1} \cdot nm^{-2}$ and 0.25 $kJ \cdot mol^{-1} \cdot Hz^{-2}$ for the NOE and coupling-constant restraints, respectively.

Results and Discussion. – The heteronuclear couplings utilized in this study are listed in *Tables 1, 2,* and *3.* The homonuclear coupling constants $^3J(NH-H\alpha)$ and $^3J(H\alpha-H\beta)$ are taken from the literature [9], while some of the heteronuclear $^3J(C'-H\beta)$ coupling constants were already determined for the diastereotopic assignment of the β-methylene protons [2].

Table 1. *Coupling Constants* [Hz] *and Corresponding* ϕ *Angles* [°] *for CsA in* $CHCl_3$ *Which Determine the* ϕ *Dihedral Angle*

Residue	$^3J(HN-H\alpha)$	Torsion [a]	$^3J(HN-C\beta)$	Torsion [b]	$^3J(C'-H\alpha)$	Torsion [c]	$^3J(C\alpha-H\alpha)$	NOE Structure [d]
MeBmt[1]	–		–		5.0	6	139.9	– 89
						113		
Abu[2]	9.9	– 138	–		–		138.8	– 97
		– 102						
MeLeu[4]	–		–		2.5	– 146	137.2	– 122
						– 6		
						– 94		
						126		
Val[5]	8.5	– 149	1.4	– 176	2.7	– 144	140.5	– 104
		51		– 20		– 5		
		69		– 100		– 96		
		– 91		56		125		

Table 1 (cont.)

Residue	^3J(HN–Hα)	Torsion [a]	^3J(HN–Cβ)	Torsion [b]	^3J(C′–Hα)	Torsion [c]	^3J(Cα–Hα)	NOE Structure [d]
MeLeu[6]	–		–		–		144.3	– 82
Ala[7]	7.4	– 156	1.4	– 176	4.3	3	138.8	– 67
		37		– 20		117		
		– 84		– 100				
		82		56				
D-Ala[8]	8.0	– 76	1.0	– 52	2.4	– 126	141.9	80
		87		106		93		
		– 44		14		6		
		152		173		147		
MeLeu[9]	–		–		2.7	– 144	140.2	– 125
						– 5		
						– 96		
						125		
MeLeu[10]	–		–		–		140.2	– 131
MeVal[11]	–		–		3.4	– 134	140.2	– 120
						– 1		
						– 106		
						121		

[a]) Values of 9.4, −1.1 and 0.4 were used for *A*, *B*, and *C* in *Eqn. 2* [7].
[b]) Values of 4.7, −1.2 and −0.2 were used for *A*, *B*, and *C* in *Eqn. 2* [7].
[c]) Values of 9.0, −4.4 and −0.8 were used for *A*, *B*, and *C* in *Eqn. 2* [7].
[d]) Values from [3a].

Table 2. *Coupling Constants* [Hz] *for CsA in* $CHCl_3$ (27°) *Which Determine* χ_1 [a])

Residue	^3J(Hα–Hβ)	^3J(Hβ–C′)	^3J(Cγ–Hα)
MeBmt[1]	6.3		0.5
Abu[2]	7.1 *R*	1.9 *R*	–
	8.0 *S*	4.7 *S*	
MeLeu[4] [b])	11.8 *R*	2.9 *R*	–
	4.2 *S*	1.8 *S*	
Val[5]	10.2	–	1.0 *R*
			3.2 *S*
MeLeu[6] [b])	10.3 *R*	7.3 *R*	
	6.0 *S*	1.5 *S*	
MeLeu[9]	11.2 *R*	–	
	4.6 *S*		
MeLeu[10]	8.2 *R*	–	
	6.5 *S*		
MeVal[11]	11.0	–	1.2 *R*
			2.5 *S*

[a]) The *R* and *S* indicate the diastereotopic assignments.
[b]) The values for ^3J(Hα–Hβ) and ^3J(C′–Hβ) were previously determined, and the β-methylene protons are diastereotopic assigned [8]. The heteronuclear coupling constants in [2] measured with a H,C-COLOC are in good agreement with the couplings determined from the HMBC spectrum.

Table 3. *$^3J(C\delta-H\beta)$ Coupling Constants Measured for CsA in $CHCl_3$ (27°) Which Determine χ_2*[a])

Residue	^3J(Cδ(pro-*S*)–Hβ) [Hz]	^3J(Cδ(pro-*R*)–Hβ) [Hz]
MeLeu[4]	6.7 *R*	2.2 *R*
	2.7 *S*	2.2 *S*
MeLeu[6]	2.6 *R*	3.0 *R*
	3.4 *S*	6.0 *S*
MeLeu[9]	5.3 *R*	2.6 *R*
	4.4 *S*	2.0 *S*
MeLeu[10]	–[b])	4.5 *R*
	–[b])	3.8 *S*

[a]) The *R* and *S* indicate the diastereotopic assignments.
[b]) Values could not be determined because of overlapping proton resonances of both δ-Me groups.

The best way to visualize the restraints from the multiple ^3J coupling constants is the energy profile of the penalty term used. These have been plotted in the *Figure* for two backbone ϕ torsions (Ala[7] and D-Ala[8]) and two side-chain torsions (χ_1 for MeLeu[6], χ_2 for MeLeu[4]). A number of points should be addressed with these figures. It is clear that restraining to a particular range of dihedral values (as is carried out in dihedral angle restraining) is not an accurate description of the information obtained from the coupling constants. The figures also indicate the importance of using more than one coupling about a single torsion. For most of the cases investigated here, the sum of all of the scalar couplings produce a more restricted range of allowed values compared with using only one *J* value.

It is interesting to note that simply calculating the expected torsions from each of the coupling constants (producing up to four answers) and then choosing those values that are closest together may not in every case produce the same minima as predicted from the sum of all of the couplings. This arises from the fact that the penalty in energy is different for each kind of coupling and dependent on the values *A*, *B*, and *C* used in *Eqn. 2*. Each scalar couplings contributes different weights to the sum of the energy profile. This is demonstrated for the ϕ dihedral angle of Ala[7]. From the calculated values in *Table 1*, an average value of 30° would be assumed, a compromise of the three couplings (*i.e.* 37°, 56°, and 3°). But from the energy profile in the *Figure, a*, it is clear that the preferred minimum is at −100°. This is not in complete agreement with the ϕ angle from the NOE structure [9] which is − 67° (arrow in *Fig., a*), but it shows that with the penalty function used here, results which are close to the NOE structure can be obtained. With variation of the force constants, the contribution from each coupling can be individually adjusted according to the accuracy and precision of the *J* value and its angular correspondence. This is an important advantage of using the *Karplus* curve directly as a penalty term in contrast to dihedral angle restraining.

The restraints from coupling constants should be separated into two categories, those of the backbone and those of the side chains. According to the refined NOE measurements, the backbone of CsA can be considered to adopt *one predominant* conformation. There is no indication from NOE-derived distances that there exist a rapidly exchanging conformational equilibrium as was observed for antamanide [25].

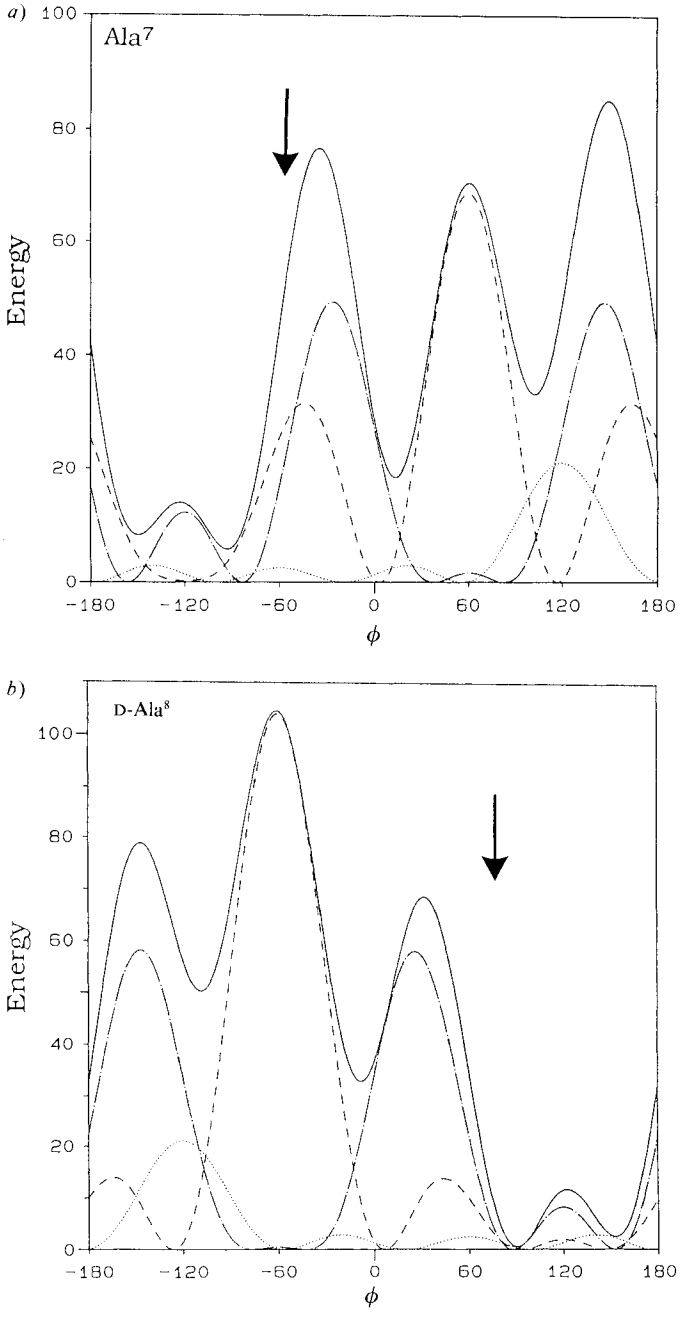

Figure. *The potential energy of the coupling constant penalty term as a function of various dihedral angles demonstrated at four selected examples.* The energy (using *Eqns. 1* and *2* with a force constant of 1 kJ mol^{-1} Hz^{-2}) is plotted for the ϕ dihedral angle of Ala[7] (*a*) and D-Ala[8] (*b*) with the ^3J(HN–Hα) (–·–·), ^3J(HN–Cβ) (· · · ·), and ^3J(C′(i – 1)–Hα) (– – –) and the sum of the functions (——) are illustrated. In *c*, the energy profile for the χ_1 of MeLeu[6] is shown for ^3J(Hα–Hβ(pro-*S*)) (· · · ·), ^3J(Hα–Hβ(pro-*R*)) (————), ^3J(C′–Hβ(pro-*R*)) (– –),

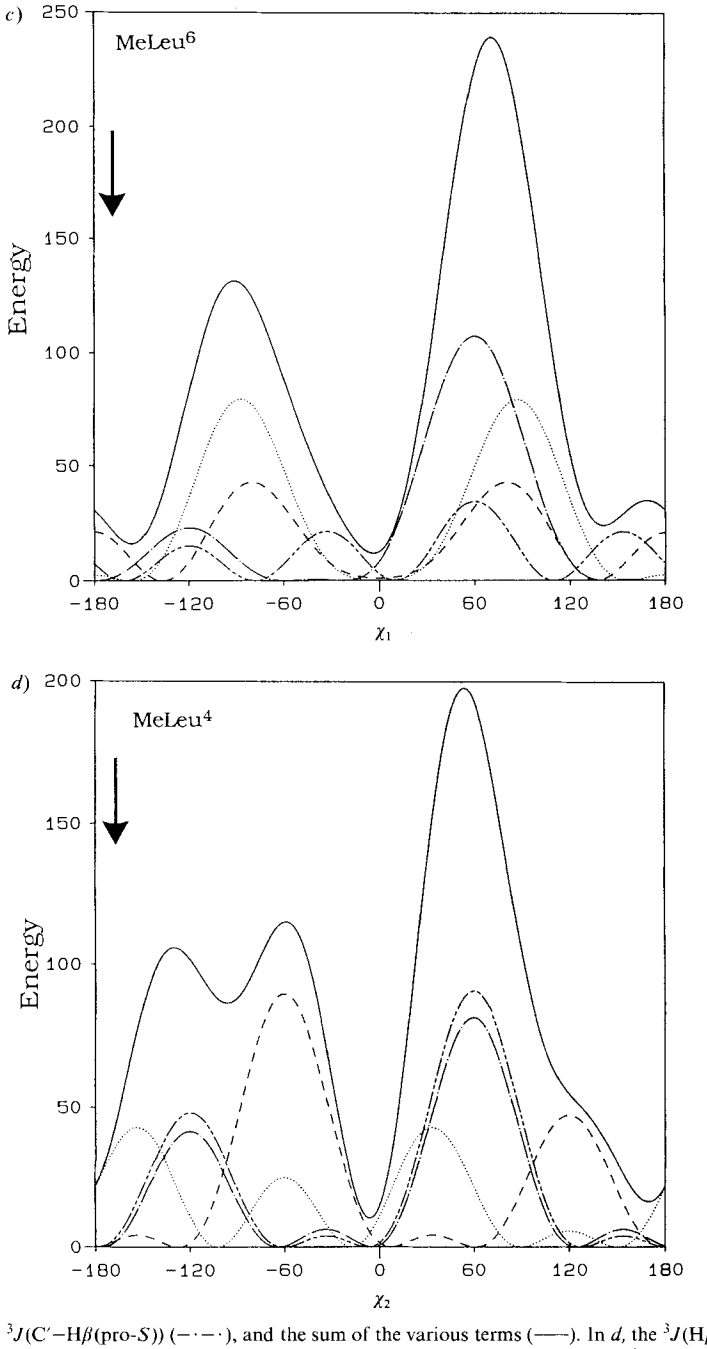

^3J(C′–Hβ(pro-*S*)) (–·–·), and the sum of the various terms (——). In *d*, the ^3J(Hβ(pro-*R*)–Cδ(pro-*R*)) (– – – –), ^3J(Hβ(pro-*R*)–Cδ(pro-*S*)) (· · · ·), ^3J(Hβ(pro-*S*)–Cδ(pro-*R*)) (– –), and ^3J(Hβ(pro-*S*)–Cδ(pro-*S*)) (–·–·) couplings and the sum of the functions (——) are shown for the χ_2 of MeLeu^4. It should be kept in mind that the minima at $\chi_1 = 0$ or $\chi_2 = 0$, which are allowed from the *Karplus* curves, are not minima in reality. This range is sterically disallowed and will be avoided from the force field. The arrow shows the results from the NOE derived structure.

The effect of the ^1J couplings on the backbone conformation was investigated by applying the restraints to both the NOE and ^3J-refined structures. Both of these starting structures are minima, or close to a minimum, as determined from the $^1J(C\alpha-H\alpha)$ couplings. The simulations including the ^1J restraints, produced no conformational differences. We must note here that the *A*, *B*, and *C* parameters described in [6] may not be appropriate for *N*-methylated residues, accounting for seven of the residues of CsA. Therefore, only four of the eleven measured $^1J(C\alpha-H\alpha)$ coupling constants are described by the correct *Karplus* equation. From preliminary examinations of a series of small model peptides, the parameters for proline need to be adjusted. A further examination for prolines and *N*-methylated amino acids is in progress and will be reported elsewhere [26].

The simulation beginning with the NOE-refined structure using the coupling constants showed no significant change during the simulation. This is not surprising as can be seen from the energy profiles shown in the *Figure*. The structure from the NOEs is already in good agreement with the coupling constants. However, starting from a structure far from the NOE-derived conformation and application of only *J*-coupling constraints illustrates that the coupling constants are not sufficient to produce the correct conformation of the molecule (*i.e.* as produced from the NOEs). Obviously, the number of restraints is not sufficient to adequately describe the structure, even though altogether 62 coupling constants were utilized.

The inadequate number of coupling constants is especially apparent for the backbone, where only three ϕ torsion angles are determined by more than one ^3J coupling constant. Each of these torsions are in agreement with the NOE structure. For the ϕ angles of the other residues, one of the other minima from the couplings is obtained from the simulation. In this test case, there are no three-bond couplings for the ψ torsions. The only restraint on this torsion comes from the one-bond coupling. It was hoped that from the three-bond couplings, the 'correct' ϕ would be obtained and then the number of possible ψ angles greatly reduced by the one-bond coupling. However, the dependence of the $^1J(C\alpha-H\alpha)$ on the ψ angle is smaller than that for the ϕ angle, as one can see from the parameters *B* and *C* in *Eqn. 3* ($B = 14.0$, $C = 4.9$).

The assumption of one predominant conformation made for the backbone of CsA is not generally valid for side chains. One approach for the analysis of side chains is to assume an equilibrium of the three ideally staggered rotamers (−60°, 180°, and 60°) and to calculate relative populations following the method of *Pachler* [27]. With limited data sets (*e.g.* homonuclear couplings and NOE restraints), this is appropriate. Another approach is to use time-dependent restraints for the couplings [28], similar to that preposed for NOEs [29]. The usefulness of this method with multiple couplings has not yet been investigated. However, with multiple couplings as have been measured here, free rotations and even significant populations of two of the rotamers can be eliminated. This is the case for MeBmt[1], Abu[2], MeLeu[4], Val[5], MeLeu[6], and MeVal[11]. Here, time-independent constraints has been used for *J* coupling, simply using a smaller force constant to allow for more mobility during the MD simulation. This is true even for the amino acids for which only two coupling constants are available (although, as discussed above, for these cases one must think in terms of relative population levels, since the constant constraints are not appropriate for such cases, *e.g.* MeLeu[9] and MeLeu[10]). In *Table 4*, the side-chain conformations from the X-ray structure, the NOE structure, and the structure derived from coupling constants are compared. The side-chain angles χ_1 and χ_2 fit with the

Table 4. *Side-Chain Dihedral Angles* [°] *of Different Structures of Cyclosporin A*

Torsion		X-Ray structure	Coupling restraints	Previous rMD[a])
MeBmt[1]	χ_1	– 166	– 101	– 77
Abu[2]	χ_1	– 178	– 78	– 70
MeLeu[4]	χ_1	51	– 91	– 151
	χ_2	54	172	– 172
Val[5]	χ_1	– 51	– 52	– 61
MeLeu[6]	χ_1	– 176	– 164	– 178
	χ_2	– 177	172	– 175
MeLeu[9]	χ_1	– 54	– 84	– 60
	χ_2	– 63	169	– 70
MeLeu[10]	χ_1	– 163	– 155	– 148
	χ_2	– 169	– 63	– 78
MeVal[11]	χ_1	53	– 78	– 60

[a]) Structure reported in [3a].

NOE structure with the exception of the χ_1 angle of MeLeu[4] and the χ_2 angle of MeLeu[9]. The reason for the agreement for the χ_1 angle of MeLeu[10] and MeVal[11] cannot be explained, since the heteronuclear couplings $^3J(H\beta{-}C')$ could not be measured for experimental reasons (low cross-peak intensities). The results here are in complete agreement with the *Pachler* analysis carried out previously for CsA [3a] which exhibits the dominating conformation to be close to the conformation obtained here.

We must conclude that without isotopic substitution, especially the amide N-atom, the determination of the conformation of peptide (and proteins) solely from coupling constants seems to be not feasible in this case. With the isotopic substitution, both the $^3J(N(i){-}H\alpha(i-1))$ and $^3J(N(i){-}C\beta(i-1))$ are readily measured, and the approach only using scalar coupling constants may produce more realistic and useful conformations. However, it must be kept in mind that the *Karplus* curves for these couplings have drawbacks. The $^3J(N(i){-}H\alpha(i-1))$ is greater than 2.0 only, when ψ is between $-20°$ and $-100°$, other ψ values produce small couplings and are, therefore, associated with a large error or cannot be measured. Worse problems are encountered with the $^3J(N(i){-}C\beta(i-1))$ coupling. In conclusion, CsA may not be a good model system, because of the seven *N*-methylated amino acids greatly reduce the number of coupling constants available for the ϕ dihedral angles.

The authors wish to thank Dr. *James Keeler* (Cambridge) for making available a program for extraction of the heteronuclear coupling constants. Financial support from the *Deutsche Forschungsgemeinschaft* and *Fonds der Chemischen Industrie* is gratefully acknowledged. *M.K.* thanks the *Fonds der Chemischen Industrie* for a fellowship.

Experimental. – *General Measurement Conditions.* All spectra are recorded at 300 K on a *Bruker-AMX500* spectrometer ($\nu_0(^1H) = 500.13$ MHz; $\nu_0(^{13}C) = 125.75$ MHz). The spectra are recorded with quadrature detection in F_1 using TPPI. The heteronuclear ^{1}H-detected experiments, except the HMBC, are run using a BIRD$_x$ pulse ($90°_x(^1H)$-*D*2-$180°_x(^1H)$,$180°_x(^{13}C)$-*D*2-$90°_x(^1H)$). The recovery delay D_4, occurring in these experiments, covers the time between the end of the BIRD$_x$ pulse and the beginning of the pulse sequence.

1. *HETLOC Spectrum.* Sequence: D_1-$90°(^1H)$-D_2-$90°(^{13}C)$-D_{10}-$180°(^1H)$-D_{10}-$90°(^{13}C)$-D_2-t_1-MLEV17-t_2. $D_1 = 172$ ms, $D_2 = 3.57$ ms, $D_{10} = 2$ µs, MLEV17 80 ms, spectral width in F_1 and F_2 4545 Hz, size 2048 data points, 512 increments, 240 scans.

2. *HMBC Spectrum.* Sequence: D_1-90°-(^{1}H)-D_2-90°(^{13}C)-D_6-90°(^{13}C)-t_1/2-180°(^{1}H)-t_1/2-90°(^{13}C)-180°(^{1}H)-t_2. $D_1 = 1.3$ s, $D_4 = 140$ ms, $D_2 = 3.57$ ms, $D_6 = 80$ ms, spectral width in F_2 is 4500 Hz in F_1 1280 Hz, size 8192 data points, 512 increments, 240 scans.

3. *Reference Spectrum.* Sequence: D_1-90°(^{1}H)-t_1-90°(^{1}H)-τ-DIPSI2-τ-90°(^{1}H)-t_2. $D_1 = 1.3$ s, τ variable delay for z filter: 3 μ, 350 μ, 700 μ, 1050 μ, 1400 μ, 1750 μ, 2100 μ, 2450 μ, 2800 μ, 3150 μ, 3500 μ. DIPSI2 80 ms, spectral width in F_1 and F_2 4500 Hz, size 8192 data points, 512 increments, 44 scans.

4. *HMQC Spectrum.* Sequence: D_1-90°(^{1}H)-D_2-90°(^{13}C)-t_1/2-180°(^{1}H)-t_1/2-90°(^{13}C)-D_2-t_2. $D_1 = 170$ ms, $D_2 = 3.57$ ms, $D_4 = 140$ ms, spectral width in F_1 17000 Hz, in F_2 4500 Hz, size 2048 data points, 384 increments, 16 scans.

REFERENCES

[1] a) M. Karplus, *J. Chem. Phys.* **1959,** *30,* 11; b) M. Karplus, *J. Am. Chem. Soc.* **1963,** *85,* 2870; c) V. F. Bystrov, *Prog. NMR Spectrosc.* **1976,** *10,* 41.

[2] H. Kessler, C. Griesinger, K. Wagner, *J. Am. Chem. Soc.* **1987,** *109,* 6927.

[3] a) H.-R. Loosli, H. Kessler, H. Oschkinat, H.-P. Weber, T. J. Petcher, A. Widmer, *Helv. Chim. Acta* **1985,** *68,* 682; b) H. Senn, B. Werner, B. A. Messerle, C. Weber, R. Traber, K. Wüthrich, *FEBS Lett.* **1989,** *249,* 113; c) P. Güntert, W. Braun, M. Billeter, K. Wüthrich, *J. Am. Chem. Soc.* **1989,** *111,* 3997; d) M. Sattler, H. Schwalbe, C. Griesinger, *ibid.* **1992,** *114,* 1126.

[4] a) M. Kurz, P. Schmieder, H. Kessler, *Angew. Chem. Int. Ed.* **1991,** *30,* 1329; b) P. Schmieder, H. Kessler, *Biopolymers* **1991,** *32,* 435.

[5] D. F. Mierke, S. Golic Grdadolnik, H. Kessler, *J. Am. Chem. Soc.* **1992,** *114,* 8283.

[6] H. Egli, W. von Philipsborn, *Helv. Chim. Acta* **1981,** *64,* 976.

[7] a) Y. Kim, J. H. Prestegard, *Proteins: Structure, Function, Genetics* **1990,** *8,* 377; b) D. F. Mierke, H. Kessler, *Biopolymers* **1992,** *32,* 1277.

[8] a) A. D. Kline, W. Braun, K. Wüthrich, *J. Mol. Biol.* **1988,** *204,* 675; b) J. M. Moore, D. A. Case, W. J. Chazin, G. P. Gippelt, T. F. Havel, R. Powls, P. Wright, *Science* **1988,** *240,* 314.

[9] H. Kessler, M. Köck, T. Wein, M. Gehrke, *Helv. Chim. Acta* **1990,** *73,* 1818, and ref. cit. therein.

[10] a) J. Keeler, D. Neuhaus, J. J. Titman, *J. Chem. Phys.* **1988,** *146,* 545; b) J. J. Titman, D. Neuhaus, J. Keeler, *J. Magn. Reson.* **1989,** *85,* 111; c) J. M. Richardson, J. J. Titman, J. Keeler, *ibid.* **1991,** *93,* 533.

[11] L. Müller, *J. Am. Chem. Soc.* **1979,** *101,* 4481.

[12] J. R. Garbow, D. P. Weitkamp, A. Pines, *Chem. Phys. Lett.* **1982,** *93,* 504.

[13] A. Bax, S. Subramanian, *J. Magn. Reson.* **1986,** *67,* 565.

[14] A. Bax, D. G. Davis, *J. Magn. Reson.* **1985,** *65,* 355.

[15] A. Bax, M. F. Summers, *J. Am. Chem. Soc.* **1986,** *108,* 2093.

[16] P. Schmieder, S. Zimmer, H. Kessler, *Magn. Reson. Chem.* **1991,** *29,* 375.

[17] A. J. Shaka, C. J. Lee, A. Pines, *J. Magn. Reson.* **1988,** *77,* 274.

[18] O. W. Sørensen, M. Rance, R. R. Ernst, *J. Magn. Reson.* **1984,** *56,* 527.

[19] a) M. T. Cung, M. Marraud, J. Neel, *Macromolecules* **1974,** *7,* 606; b) C. A. G. Haasnoot, F. A. A. M. de Leeuw, H. P. M. de Leeuw, C. Altona, *Tetrahedron* **1980,** *36,* 2783.

[20] J. P. Rychaert, C. Cicotti, H. J. C. Berendsen, *J. Comput. Phys.* **1977,** *23,* 327.

[21] W. Jorgensen, J. M. Briggs, M. L. Contreras, *J. Phys. Chem.* **1990,** *94,* 1683.

[22] D. F. Mierke, H. Kessler, *J. Am. Chem. Soc.* **1991,** *113,* 9466.

[23] W. F. van Gunsteren, H. J. C. Berendsen, Groningen molecular simulation library manual (GROMOS) (Biomos B.V., Groningen, 1987).

[24] H. J. C. Berendsen, J. P. M. Postma, W. F. van Gunsteren, A. DiNola, J. R. Haak, *J. Chem. Phys.* **1984,** *81,* 3684.

[25] a) H. Kessler, C. Griesinger, J. Lautz, A. Müller, W. F. van Gunsteren, H. J. C. Berendsen, *J. Am. Chem. Soc.* **1988,** *110,* 3393; b) H. Kessler, A. Müller, K.-H. Pook, *Liebigs Ann. Chem.* **1989,** 903; c) H. Kessler, J. W. Bats, J. Lautz, A. Müller, *ibid.* **1989,** 913; d) Z. L. Madi, C. Griesinger, H. Kessler, *J. Am. Chem. Soc.* **1990,** *112,* 2908.

[26] S. Golic Grdadolnik, H. Kessler, in preparation.

[27] a) K. G. R. Pachler, *Spectrochim. Acta* **1963,** *19,* 2085; b) K. G. R. Pachler, *ibid.* **1964,** *20,* 581.

[28] A. E. Torda, R. M. Brunne, T. Huber, H. Kessler, W. F. van Gunsteren, submitted to *J. Biomol. NMR.*

[29] A. E. Torda, R. M. Scheek, W. F. van Gunsteren, *Chem. Phys. Lett.* **1989,** *157,* 289.